Experimental and analytical analysis of vaned savonius turbine performance under different operating conditions

Grönman Aki, Tiainen Jonna, Jaatinen-Värri Ahti

DOI: 10.1016/j.apenergy.2019.05.105

Experimental and Analytical Analysis of Vaned Savonius Turbine Performance under Different Operating Conditions

Aki Grönman*, Jonna Tiainen, Ahti Jaatinen-Värri

LUT University, School of Energy Systems, Laboratory of Fluid Dynamics, P.O. Box 20, 53851 Lappeenranta, Finland

Abstract

Global energy production is shifting towards more distributed technologies, where power generation takes place close to people. A vaned Savonius wind turbine is one of the possible solutions, which can fulfil the requirements of being simultaneously reliable, safe and non-disturbing. One challenge is that when the size of the turbine becomes smaller and the wind velocity is low, the Reynolds number effects begin to deteriorate the performance. Public literature lacks detailed information about how the turbine performance and internal flows change in these conditions. In this work, a vaned Savonius turbine is tested in a wind tunnel with seven Reynolds numbers and several tip-to-speed ratios. The measurements include both the turbine performance and the static pressures inside the vane passages. All experiments are also conducted separately for the stator only configuration to evaluate the effects of stator-rotor interaction. The main results are: (1) a new Reynolds number-dependent performance prediction correlation is developed with an achievable accuracy of ±5%, (2) Savonius turbine power coefficient follows the trend of kinetic compressors relatively well and due to the changing Reynolds number, an over 20% drop in vaned turbine performance can be observed, (3) the Reynolds number affects performance through friction and flow separations, but the vane passage pressure distribu-

*Corresponding author
Email address: gronman@lut.fi (Aki Grönman)

tions are not affected and (4) tip-to-speed ratio affects the vane passage pressure distribution via stator-rotor interaction. It is also suggested that the nominal tip-to-speed ratio should be kept relatively low in the design phase to minimise the negative effects of stator-rotor interaction.

Keywords: Savonius rotor, wind turbine, renewable energy, Reynolds number, off-design

---

Nomenclature

A: rotor swept area [m^2]

c: vane chord [m]

C_P: power coefficient [-]

C_P, ref: power coefficient at data sets' maximum Reynolds number [-]

D: rotor diameter [m]

n: constant in Reynolds number effect equation [-]

Δp: relative pressure [Pa]

R: rotor radius [m]

Re: Reynolds number [-]

T: torque [Nm]

V: velocity [m/s]

V_x: axial velocity [m/s]

V_∞: free-stream velocity [m/s]

δ: boundary layer thickness [m]

ρ: density [kg/m^3]

λ: tip-to-speed ratio [-]

μ: dynamic viscosity [Pa s]

ω: angular speed [rad/s]

Abbreviations

HAWT: horizontal axis wind turbine

VAWT: vertical axis wind turbine

1. Introduction

Savonius wind turbines offer an alternative for sustainable urban energy production in the ongoing energy transition process, having relatively low noise emission compared to H-rotor and horizontal axis wind turbines (HAWTs). This behaviour is connected to the lower tip-to-speed ratio, which is further directly proportional to the emitted sound pressure level. In addition, the lower sensitivity for highly transient urban wind conditions of vertical axis wind turbines (VAWTs) favour their use over HAWTs, for example, in densely built urban areas.

There are three reported benefits that a vane system around a Savonius turbine can produce: the first is that the possible flicker-caused annoyance is expected to decrease, the second is the improved self-starting capability and the third is the improved performance. The lower flicker-related annoyance is explained by restricting or closing visual access to the rotating blade, as discussed by Grönman et al. [1]. The improved self-starting capability is related to the flow accelerating effects of the vane ring or shielding the returning blade. Mohamed et al. [2] reported that a self start was enabled at any rotor position for their obstacle-shielded Savonius turbine. By adding an omnidirectional guide vane, the 7.35 m/s self-start wind speed of an H-rotor was reduced to 4 m/s in a study by Chong et al. [3]. In their work related to a Sistan turbine, Chong et al. [4] reported that the power augmentation guide vanes enabled rotor self-starting.

The performance improvement, on the other hand, is related to guiding the flow to the advancing blade and simultaneously keeping the flow away from the returning blade. This means that more kinetic energy is available for producing positive power and less when producing negative power. In addition, the study by Grönman et al. [1] suggested that the circulating flow system inside the vane ring can be beneficial from the rotor's performance point of view. Alexander and Holownia [5] were the first to show that flat plate shielding can improve the performance of a Savonius turbine. Later, a similar finding was made by

Mohamed et al. [2] by using obstacle shielding. A study by Shahizare et al. [6], showed that with an optimal vane design, the performance of an H-rotor can be improved. Also, Nobile et al. [7] predicted that the performance of an H-rotor is improved with a vane system. Positive turbine performance changes were also found by Tartuferi et al. [8] in their experimental study for a self-orienting curtain system. Similar results are presented by Altan and Atilgan [9] for an upstream shielded Savonius turbine. In addition, a study by Irabu and Roy [10] reported a positive influence on the performance when a guide box was used. In a numerical and experimental study, Korprasertsak and Leephakpreeda [11] found that adding a symmetric guide vane ring around a two-bladed Savonius rotor improves its power coefficient significantly. Yet it should be noted that the performance improvement can sometimes only occur in a small number of the tip-to-speed ratio values tested, as was the case with Hayashi et al. [12]. This emphasises the importance of the design process and matching the vane and rotor for different operating conditions. Recently, Chong et al. [13] tested an upstream deflector in a cross-axis wind turbine that consisted of both an H-type rotor and of horizontal blades. They were able to improve the performance over a VAWT and showed the significance of the deflector angle for the overall performance.

Despite its benefits, a downstream vane ring can negatively influence the rotor airflow flow as was discussed by Takao et al. [14]. Later, Grönman et al. [1] also discussed how a vane ring without a geometrical throat should reduce its negative effect on the exiting flow. They also discussed how the increased physical size of the turbine can be a challenge in places where the size is a decisive factor.

In addition to a vane ring or different obstacle-shielding approaches, the Reynolds number (Re) can have a dramatic influence on the performance of rotating machinery. For example, in gas turbine technology, the advent of micro gas turbines is partly hindered by the relatively low performance of the turbomachinery components due to the Reynolds number-related losses. In terms of power, Galanti and Massardo [15] suggested that the drop in performance ac-

celerates when the gas turbine's nominal power goes below approximately 100 kW. It has also been shown that the performance of a kinetic compressor decreases drastically after passing the critical chord Reynolds number of 200 000 [16] (referred to as the low Reynolds number area). The Reynolds number can be affected by operating conditions or by the changes in the machine's characteristic dimensions. However, the influence of the Reynolds number variation method does not influence the observed performance trends except in those cases where the relative clearances need to be changed due to manufacturing limits, as discussed by Tiainen et al. [17]. From the fluid dynamic point of view, the main loss mechanism, which is affected while the Reynolds number changes, is the boundary layer loss [18], indicating that the role of the wetted area becomes important. Also of paramount importance is the finding that the relative significance of the vortical flow structures do not change while the Reynolds number varies.

Several researchers have shown the general trend that a decreasing Reynolds number has a detrimental influence on vaneless Savonius turbine performance; however, a detailed analysis that examines the effect of different Reynolds number levels is still missing. From the flow phenomena point of view, it has also been discussed how the Reynolds number affects the flow separation in the rotor buckets by causing earlier separation from the back side of the bucket when the Reynolds number decreases [19]. A review article by Akwa et al. [20] presented how the torque coefficient of a Savonius turbine decreases over a variety of tip-to-speed ratios as the Reynolds number decreased. Similar results were also presented by Hayashi et al. [12] when they performed experimental research on one- and three-stage Savonius turbines. Mostly similar results were also reported by Blackwell et al. [19] for the different Savonius rotors tested. Al-Faruk and Sharifian [21] presented the maximum power coefficient for four Reynolds numbers for their swirling two-bladed Savonius turbine, showing an accelerating trend towards a steeper drop in performance as the Reynolds number decreases. In a study of Roy and Saha [22], several different Savonius turbines were tested. Their results indicated that the maximum power coefficient increases from Re

= 150 000 to Re = 120 000 but decreases when the Re < 120 000. Kamoji et al. [23] examined the performance of a helical Savonius turbine with 57 700 $\leq Re \leq$ 202 000, and their results showed that the maximum power coefficient decreases as the Reynolds number decreases. The observed general trend was also similar over a wide range of tip-to-speed ratios. In another study, Kamoji et al. [24] experimentally studied a modified two-bladed Savonius rotor, and they found that the peak power coefficient decreases when the Reynolds number decreases to the range 80 000 $\leq Re \leq$ 150 000. Also, Mercado-Colmenero et al. [25] concluded that the maximum power coefficient increases with an increasing Reynolds number for different tested Savonius rotors. In addition, their results suggested that the position of maximum power coefficient moves towards a higher tip-to-speed ratio when the Reynolds number increases. Wang and Yeung [26] discussed how the Reynolds number effect might be minimal for drag-based turbines, which make them suitable for micro-scale energy production. However, they were not able to identify the cause of their finding. Han et al. [27] investigated several miniature 3D-printed Savonius turbines with the maximum electrical power of 0.305 W. In terms of energy conversion efficiency, a decreasing Reynolds number did not always lead to lower performance. This phenomenon could be, for example, partly due to the changing tip-to-speed ratio during the measurements. In another study by Zhao and Han [28], it was also noticed that the turbine orientation affected its performance at different Reynolds numbers.

The previous work by the authors [1] revealed the fundamental fluid dynamic behaviour in a vaned Savonius turbine and included detailed experimental and numerical analysis using one Reynolds number and tip-to-speed ratio. To the authors' knowledge, the work conducted by Burlando et al. [29] is the only other study that presents static pressure measurements inside a Savonius turbine stator. However, in their work, there is no experimental data for a case where the rotor is also included.

From the presented background, it is noticeable that the Reynolds number plays a significant role in turbine performance, but its role has not yet been

examined in detail in the case of a vaned Savonius turbine. In addition, the understanding about the internal flow phenomena and their importance from performance and design points of view are not well covered either. The availability of experimental data is also very limited. Therefore, this work aims to fill the mentioned research gaps and pushes the research in vaned Savonius turbines a step forward. So far, the most complete analysis of this turbine type's performance and internal flow phenomena in different operating conditions is presented. It provides new experimental data with seven Reynolds numbers and several tip-to-speed ratios. The results are presented both with and without the stator-rotor interaction, which means that the research has applicability also in other rotor designs. In addition, the effects of the Reynolds number on the performance of different Savonius turbines are analysed in detail in order to extend the analysis. The key novelties of the current study are as follows:

1. A new Reynolds number-dependent correlation for vaned Savonius turbine performance prediction is developed.
2. The role of the Reynolds number is revealed for a vaned Savonius turbine from performance and stator-rotor interaction points of view.
3. The role of tip-to-speed ratio is revealed for a vaned Savonius turbine from performance and stator-rotor interaction points of view.
4. Design recommendations are presented for improved designs.

The article is constructed so that after presenting the turbine design and experimental setup in Section 2, the turbine performance is examined in the beginning of Section 3.1. At the end of the Section 3.1, the general effects of the Reynolds number on the normalised power coefficient are evaluated with other available designs. In Section 3.2, a new correlation for calculating the torque coefficient for a vaned Savonius turbine is presented and validated. The next Section, 3.3, presents how the static pressure distributions are affected by the Reynolds number and tip-to-speed ratio, both with and without the rotor. In Section 4, conclusions and summary of the key findings are presented.

2. The experimental setup

In the experimental campaign, a vaned three-bladed Savonius turbine was used. Additive manufacturing was used to produce the stator vanes and the rotor blades from polyactid. The rotor has an open centre section, and the vanes do not have a geometrical throat which would restrict the flow. The main vane design principle was that the vanes should guide the flow to the advancing blade, and they should simulataneously limit the flow that interacts with the returning blade. A more detailed description of the turbines' design principles is given by Grönman et al. [1]. The main design parameters are presented in Table 1, and a schematic two-dimensional top view of the turbine is shown in Fig. 1, which also presents the approximate static pressure tapping locations at the bottom of the vane passages.

Table 1: The main turbine design parameters.

Vane outer diameter [m]	0.750	Vane inner diameter [m]	0.594
Rotor outer diameter [m]	0.580	Rotor centre diameter [m]	0.203
Vane height [m]	0.326	Rotor blade height [m]	0.300
Vane aspect ratio (h/c) [-]	2.47	Rotor aspect ratio (h/d) [-]	0.52
Number of stator vanes [-]	16	Number of rotor blades [-]	3
Solidity [-]	0.88	Reynolds number [-]	910 100

A closed-loop, Göttingen-type wind tunnel [30] was used in the experiments. The hexagonal test section has an area of 3.67 m^2 and a length of 4.41 m with 2 m maximum height and width, respectively. The intensity of turbulence is below 0.19%. In Fig. 2, the turbine is shown installed during the tests, and compared to the test sections' cross-sectional area, its projection causes a blockage of 6.7%. Since the turbine is not located vertically at the centre of the test section, the previous study by Grönman et al. [1] examined the influence of the turbine's

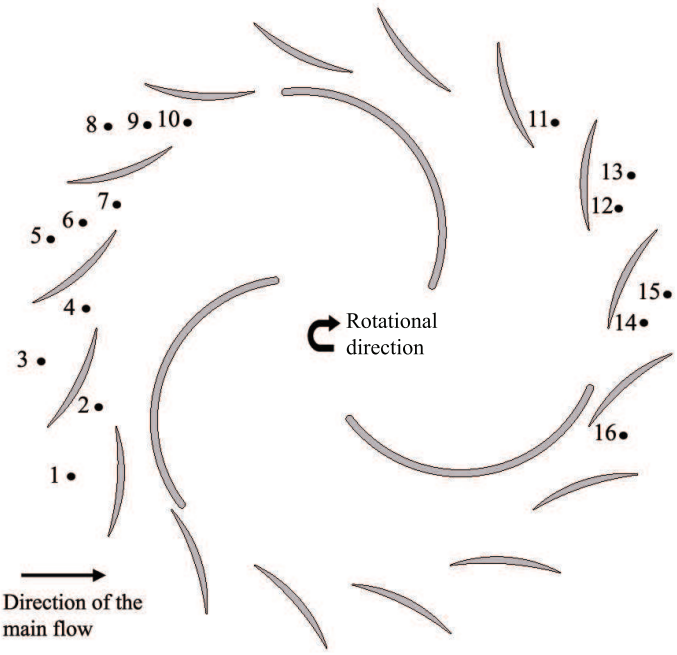

Figure 1: A schematic presentation of static pressure tapping positions. See Appendix 1 in Grönman et al. [1] for exact tapping locations.

vertical location on the results and found that its effect is insignificant.

Seven Reynolds numbers were measured in the range 221 600 $\leq Re \leq$ 886 300, while the tip-to-speed ratio was measured in the range $0.39 \leq \lambda \leq 0.94$. All cases were measured both with the stator only, and with the stator and the rotor included simultaneously in order to isolate the influence of stator-rotor interaction from the results. During the experiments, the turbine rotational speed was varied by increasing the load from the generator, while keeping the flow velocity and Reynolds number constant for each measured performance curve.

Calibrated pressure and temperature measurements were used in the experimental campaign. The flow velocity was measured in the wind tunnel by a pitot tube, which had a maximum error of $\pm 1\%$. A thermocouple with an accuracy of ± 1 K was used to measure the air temperature before the test section in a

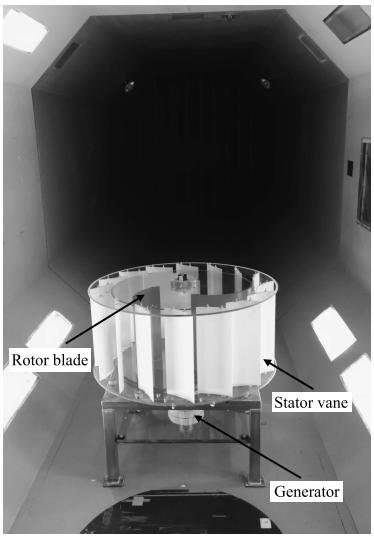

Figure 2: The studied turbine during the experiments in the wind tunnel [1].

settling chamber. The pressure measurent accuracy at the settling chamber was estimated to be ±10 Pa. Figure 1 shows the approximate positions of the 16 pressure tappings that were installed in the bottom plate of vane passages; the accurate tapping positions are presented by Grönman et al. [1]. These measurements were conducted with a 16-channel differential pressure sensor at a 10 Hz frequency for each operating point, for 60 seconds, with an error estimate of ±10 Pa.

A calibrated torque sensor NCTE2000-5NM was installed next to the generator, below the turbine, with an estimated error of ±1%. The generator frequency was used to calculate the rotor speed with an accuracy of ±24 rpm, which follows the estimate of Grönman et al. [31].

The turbine performance data is presented with four non-dimensional parameters: the tip-to-speed ratio, power coefficient, torque coefficient and the Reynolds number. In addition, in order to include the effects of the wind tunnel, the correction method of Alexander and Holownia [5] is utilised. The tip-to-speed ratio λ is defined based on the measured angular velocity ω, rotor radius

R and the free stream velocity V_∞ as follows

$$\lambda = \frac{\omega R}{V_\infty}, \tag{1}$$

whereas the measured torque T is used in the calculation of the power coefficient

$$C_P = \frac{T\omega}{0.5\rho A V_\infty^3}. \tag{2}$$

and the torque coefficient defined as

$$C_T = \frac{T}{0.5\rho A R V_\infty^2}. \tag{3}$$

The Reynolds number is calculated based on the rotor diameter D in order to be able to compare it directly with the non-vaned designs as follows:

$$Re = \frac{\rho V_\infty D}{\mu}. \tag{4}$$

The error of C_P is $\pm 3.2\%$ and the error of C_T is $\pm 2.3\%$. The parameter $C_T/Re^{0.27}$ is explained in section 3.2, and it has an error of $\pm 2.3\%$.

3. Results

3.1. Turbine performance

As has been previously discussed, the change in a Reynolds number affects the performance of the rotating machine. Figures 3 (a) and (b) show that the turbine operating curve is shifted towards lower power and torque coefficients when the Reynolds number decreases. The results also give a possible, but very weak, indication that when the Reynolds number decreases, the peak in the power coefficient curve could be reached at a higher tip-to-speed ratio. This suggestion is made since, in general, the C_P curves seem to start bending from a linear curve shape with higher tip-to-speed ratios when the Reynolds number decreases. If this phenomenon proves true, it can be explained by the relatively weaker stator-rotor interaction at low Reynolds numbers, which means that the vanes accelerate the flow relatively more when the rotor rotates at lower

speed. The suggested trend is opposite to what Mercado-Colmenero et al. [25] found for different vaneless Savonius designs. Therefore, more data should be available in order to be able to draw conclusions. In comparison with other existing research, the peak power coefficient value was found at $\lambda = 0.48$ by Pope et al. [32] for the no-tab nine-vane and five-rotor blade Zephyr turbine, which is considered to be closest to the one examined here geometry-wise. In terms of measurement error, the observed C_P differences at different Reynolds numbers are generally larger than the calculated uncertainty.

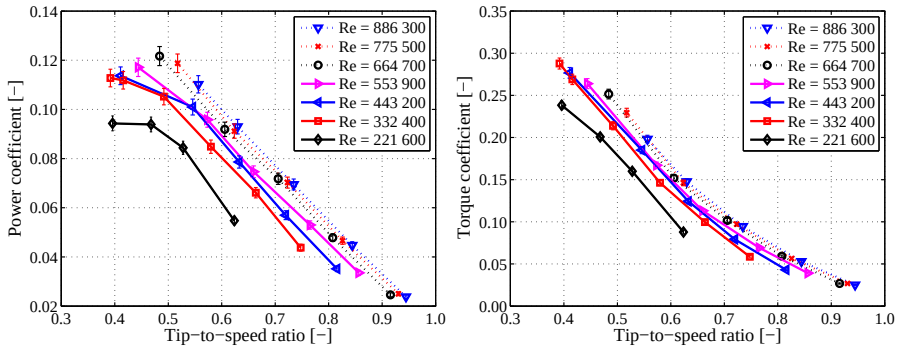

(a) (b)

Figure 3: The effect of Reynolds number on power coefficient (a) and torque coefficient (b).

The effect of the Reynolds number on the Savonius turbine power coefficient seems to roughly follow the curve shape of kinetic compressor efficiency, as presented in Fig. 4 for qualitative comparison. However, the critical value for the low Reynolds number area cannot be determined with the available data. The presented data is normalised separately for each data set by its power coefficient at the maximum Reynolds number. The prediction is made by the method of Dietmann and Casey [16], which uses the flat plate assumption. Quantitavely, it is noticeable that for the vaned Savonius turbines, the Reynolds number change can cause a more than 20% drop in power coefficient. In general, the similar curve shapes can be explained by the important role of increasing boundary layer thickness as a function of a decreasing Reynolds number. Although the

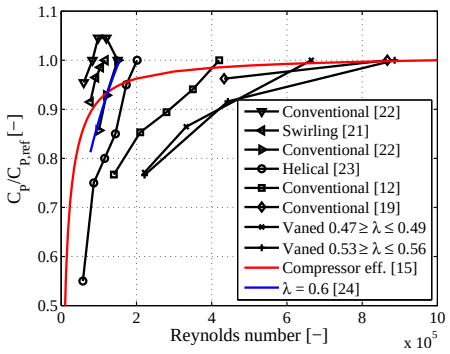

Figure 4: The effect of the Reynolds number on the normalised power coefficient with different Savonius designs. For comparison, a predicted curve shape is presented for a centrifugal compressor's relative efficiency change using the method of Dietmann and Casey [16]. Also, a curve is presented for correlation with the work of Kamoji et al. [24] where $\lambda = 0.6$.

secondary flow structures may change between different turbines, the fundamental cause for the performance degradation is the changes in viscous boundary layer losses, as discussed by Tiainen et al. [18].

3.2. Torque coefficient correlation

In this section, an approach similar to the one presented first by Kamoji et al. [24] and later by Mercado-Colmenero et al. [25] for vaneless Savonius turbines is chosen in order to develop a correletion between torque coefficient and tip-to-speed ratio for the current vaned Savonius turbine. Rotorwise, the main difference to those presented by Kamoji et al. and Mercado-Colmenero et al. is that the current rotor has three blades, and the rotor has a constant radius. On the other hand, the role of the stator-rotor-stator interaction plays a certain role in the flow physics. In addition, the Reynolds number is clearly higher in this work for all the cases. In their work, Kamoji et al. [24] found a nearly linear dependence between $C_T/Re^{0.3}$ in the following form:

$$\frac{C_T}{Re^{0.3}} = -0.0107\lambda + 0.0149 \tag{5}$$

when $\lambda \geq 0.6$ and $77\,600 \leq Re \leq 155\,000$. Later, Mercado-Colmenero et al. [25] also found a similar general dependency of C_T/Re^n for three different twisted

and vertically varying diameter Savonius rotors. Of their results, one was linear and two others followed a second-order polynomial shape. The constant n was 0.3 for two rotors and 1.5 for one rotor.

By using the $C_T/Re^{0.3}$ dependency as the initial condition, a new correlation was developed for a vaned Savonius turbine by maximising the coefficient of determination. The following formulation was found to yield a coefficient of the determination value of 0.994:

$$\frac{C_T}{Re^{0.27}} = 0.0231\lambda^2 - 0.0459\lambda + 0.0235, \tag{6}$$

when $0.39 \leq \lambda \leq 0.94$ and $221\ 600 \leq Re \leq 886\ 300$. Figure 5 (a) compares the prediction with the experimental data and shows that the majority of the data lies between the $\pm 5\%$ error curves, which is considered as a good validation for the model's accuracy. The most notable phenomenon is that the curve shape is not linear, as it was with the modified vaneless Savonius of Kamoji et al. [24]; instead, the curve follows a second-order polynomial shape, such as that found in the study by Mercado-Colmenero et al. [25]. The presented correlation is also capable of capturing the experimental performance with good accuracy. Figure 5 (b) compares the experimental data with the predicted power coefficients, where the curves are extrapolated until $\lambda = 0.2$ with dashed lines. Except for the one outlier at Re=221 600, the model prediction follows the experimental data reasonably well, and suggests that the prediction is valid for the examined Reynolds number range.

Two reasons for the differences in the observed correlation curve shape are considered. The first is the operational Reynolds number and the other is the interaction between the vane ring and the rotor. Since the results of Kamoji et al. [24] and Mercado-Colmenero et al. [25] were valid for lower Reynolds numbers than the current study examined and different correlation curve shapes were noticed, the Reynolds number does not explain the differences in the lower Reynolds numbers. In order to have a broader overview, the analysis was extended into higher Reynolds numbers by analysing the experimental data of

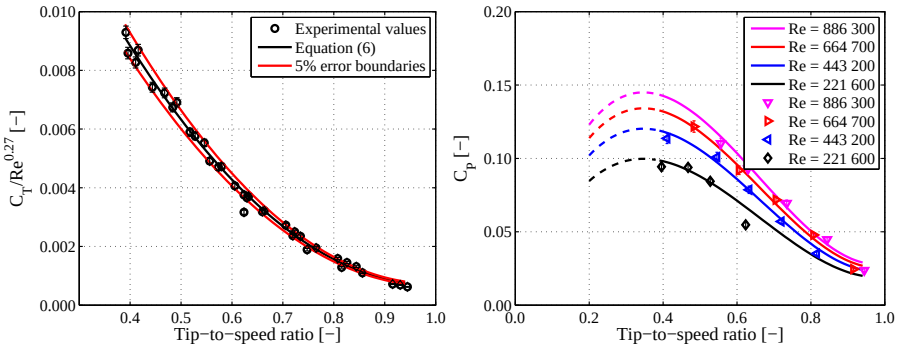

(a) (b)

Figure 5: The validation of the new correlation in Eq. 6 (a) and the validation of the power coefficient prediction (b). The dashed lines are extrapolated values outside the validity region.

Blackwell et al. [19]. Two sets of measurements were chosen: one with three rotor blades and the other with two rotor blades, with both rotors examined in a range of 432 000 $\leq Re \leq$ 867 000. The linear behaviour of C_T/Re^n was found for both the cases with three blades with $0.36 \leq \lambda \leq 1.40$ and for two blades with $0.44 \leq \lambda \leq 1.42$, for $n = 0.13$ and $n = 0.10$ respectively. These correlations, Eq. 6 and the different correlation curve shapes found at lower Reynolds numbers, are considered clear indications that the Reynolds number level does not explain the observed curve shapes. From the study of Mercado-Colmenero et al. [25], it can be found that the non-linear behaviour of the curve fits and weaker vortex structures and weaker low velocity areas take place simulataneously. Therefore, it is suggested that the stator-rotor interaction and its influence on the flow separations and vortical structures could be the root cause for the observed non-linear trend seen in Fig. 5 (a).

3.3. Static pressure distributions

3.3.1. The effect of the Reynolds number

Stator-rotor interaction has an important role in the static pressure distributions at different Reynolds numbers, as presented in Figs. 6, 7 and 8. These results are presented for tip-to-speed ratio values in the range $0.53 \leq \lambda \leq 0.56$,

but similar results are also observed in the range $0.47 \leq \lambda \leq 0.49$. The inclusion of the rotor causes differences in the vane passage pressure distributions by increasing the pressures in general upstream from the rotor, especially at the passage exit and in the middle, due to back pressure caused by the passing rotor. In general, the absolute changes in pressure values are greater when the Reynolds number increases due to stronger stator-rotor interaction, but the trends remain similar, although, especially at the lowest Reynolds number, the differences are inside the experimental error.

At the more unsteady part of the vane ring downstream of the rotor, the trends of the pressure distributions change when the stator-rotor interaction is included in the analysis. Similarily with the upstream results, the trends are again comparable, although the absolute values change more when the Reynolds number increases. The observed change in the trends indicates change of the exit flow paths towards the upper rear part of the vane ring (measurement points 11-13) when the rotor is included. The reason for the decreasing downstream pressure levels while the Reynolds number increases is expected to be due to the lower base pressure in the vane ring wake, which also allows the flow in the upstream vane passages to expand into lower pressure.

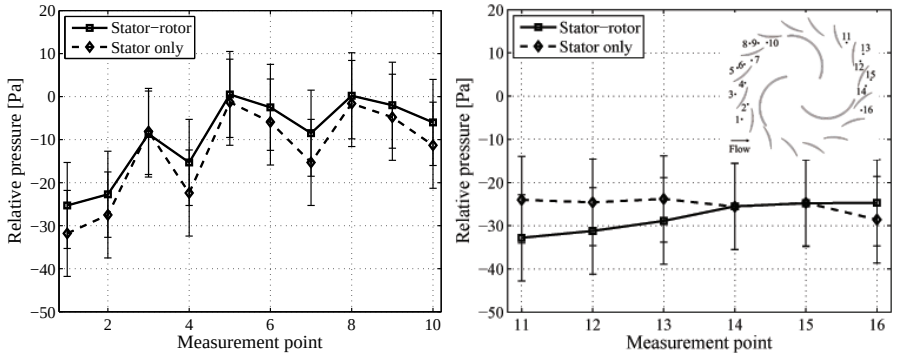

(a) (b)

Figure 6: The effect of stator-rotor interaction on relative static pressure at the upstream measurement points (a) and downstream measurement points (b). The operating Reynolds number is 221 600 and the tip-to-speed ratio is 0.53.

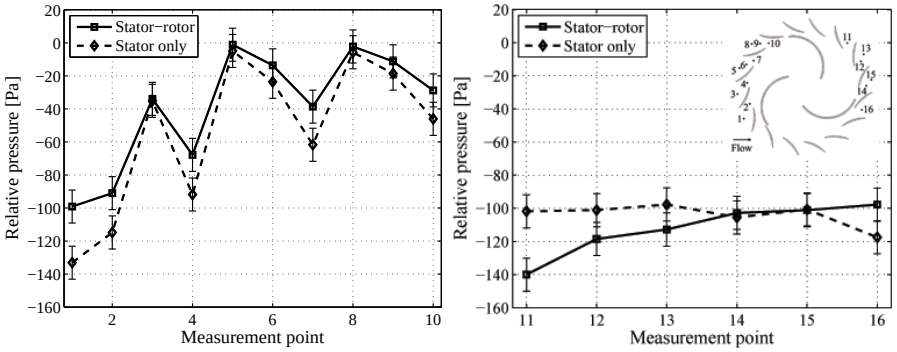

(a) (b)

Figure 7: The effect of stator-rotor interaction on relative static pressure at the upstream measurement points (a) and downstream measurement points (b). The operating Reynolds number is 443 200 and the tip-to-speed ratio is 0.55.

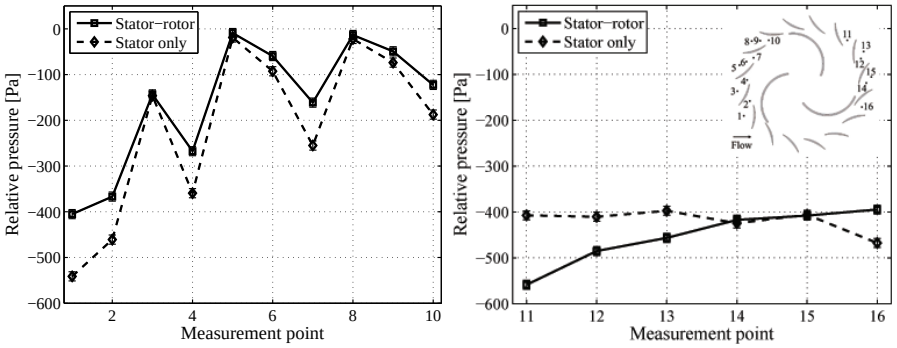

(a) (b)

Figure 8: The effect of stator-rotor interaction on relative static pressure at the upstream measurement points (a) and downstream measurement points (b). The operating Reynolds number is 886 300 and the tip-to-speed ratio is 0.56.

In terms of relative changes, the stator-rotor interaction seems to play a greater role than the Reynolds number. Figures 9 and 10 illustrate the effects of the Reynolds number and stator-rotor interaction on the relative velocity change at the upstream and downstream parts of the turbine. It can be observed that with the rotor inlcuded, the upstream measurements show differences in

the passages where the flow is accelerated (measurement points 3-10). It is worth noting that the differences are inside the error bars; however, the previous analysis of Figs. 6-8 showed that the trends are systematic at all Reynolds numbers. These noticed differences are due to the interaction between the stator and the rotor, whereas without the rotor, when the Reynolds number is the main difference between the cases, the velocity changes are practically identical.

At the downstream side of the turbine (shown in Fig. 10), where the interactions with the upstream flow make it more challenging to isolate the Reynolds number-related phenomena, there are no clear trends when the rotor is included, but without the rotor, the Reynolds number change seems to affect the distribution, especially when the lowest measured Reynolds number case is considered. No specific reason for this observed behavior was found, but it could be due to the non-linear dependence of the drag caused by the vane ring and the Reynolds number, which is typical for different obstacles in the flow.

Previous paragraphs discussed that the role of the Reynolds number is smaller than the role of the tip-to-speed ratio when the vane ring performance is examined. It is known that the decrease in the Reynolds number increases the boundary layer thickness and thus affects the effective flow area in vane passages, and through the continuity equation, the flow velocity is affected. Also, the state of the boundary layer (laminar or turbulent) influences its thickness dramatically. In order to get more insight into the role of the boundary layer, the following simplified boundary layer thickness δ analysis was performed with the laminar flat plate assumption of Schlichting [33] as follows:

$$\delta = \frac{5.0c}{\sqrt{Re}}, \tag{7}$$

where the Reynolds number is defined based on the vane chord c. The laminar boundary layer thickness estimation is justified, since the vane chord Reynolds numbers vary approximately between 50 000 and 200 000, which are mostly below the flat plates' critical limit of 200 000. In addition, the inlet turbulence intensity is very low during the measurements, which delays the boundary layer

transition process. As a result of the analysis, it was found that the theoretically estimated boundary layer thickness is approximately doubled for a single vane passage (the difference between the minimum and maximum Reynolds numbers). In a theoretical closed system, this difference would increase the flow velocity by approximately 5-6%. However, in the studied open flow system this change causes a slightly higher pressure loss, which means that less mass flow goes through the turbine. Therefore, the overall thicker boundary layers in vane and rotor surfaces are seen in decreased performance due to increased viscous losses in Fig. 3 (a) and (b), as was previously discussed.

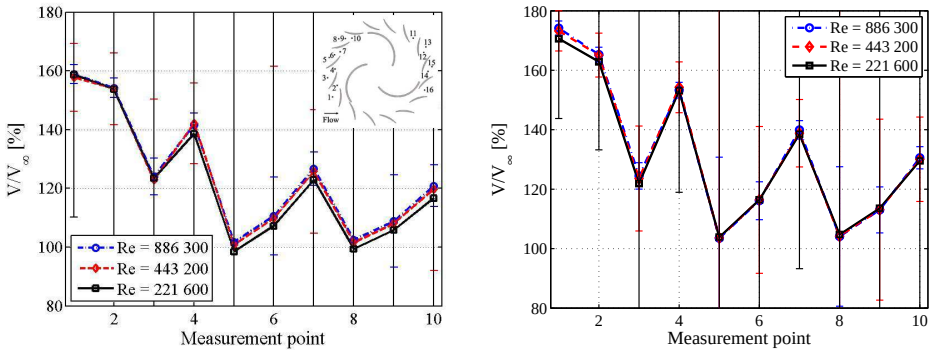

Figure 9: Velocity change relative to the free-stream value at the upstream part of the turbine with the stator-rotor interaction (a) and with the stator only (b).

3.3.2. The effect of the tip-to-speed ratio

With varying tip-to-speed ratios, the stator-rotor interaction generally has a different effect on the flow field depending on if the analysis is made on the upstream or downstream side of the vane ring. In Fig. 11 (a) to (d), the pressure distributions in accelerating vane passages approach those without the rotor when the operating point moves towards lower tip-to-speed ratios due to weaker interaction between the stationary and the rotational parts. The only difference is that at the lowest Reynolds number, the point where the maximum power coefficient is first reached ($\lambda = 0.47$), the pressure distribution is also

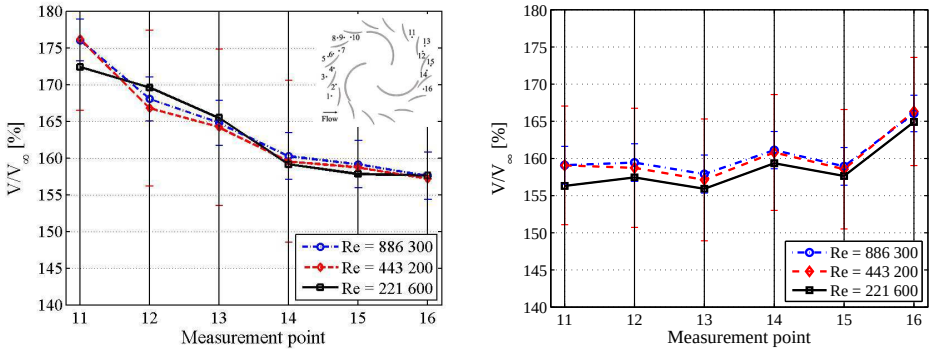

Figure 10: Velocity change relative to free-stream value at the downstream part of the turbine with the stator-rotor interaction (a) and with the stator only (b).

closest to the case without the rotor. Due to the lack of data at the maximum power coefficient at other Reynolds numbers, it cannot be said if this is due to the change in rotor performance or if it is due to measurement error, since the differences lie inside the error bars.

At the downstream part of the turbine, the effect of the tip-to-speed ratio is opposite to the upstream behaviour. Figure 12 (a) to (d) illustrates these effects at measurement points 11 to 16. In general, measurement points 14 and 15 stay relatively close to the stator-only case despite the values of Reynolds number or tip-to-speed ratio, but when the tip-to-speed ratio approaches 0.9, measurement points 12 and 13 also move closer to the case without the stator-rotor interaction, indicating changes in the downstream flow distribution. One explanation for these changes could be the development of the rotor secondary flows when the tip-to-speed ratio increases and the performance decreases. A study by Torresi et al. [34] suggested that for an open Savonius rotor, when the tip-to-speed ratio increases, the vortex that is generated by the advancing rotor is squished by the same rotor. This also means that the flow that exits the rotor is less vortical than it is at lower tip-to-speed ratios and this could explain the trend noticed in Fig. 12.

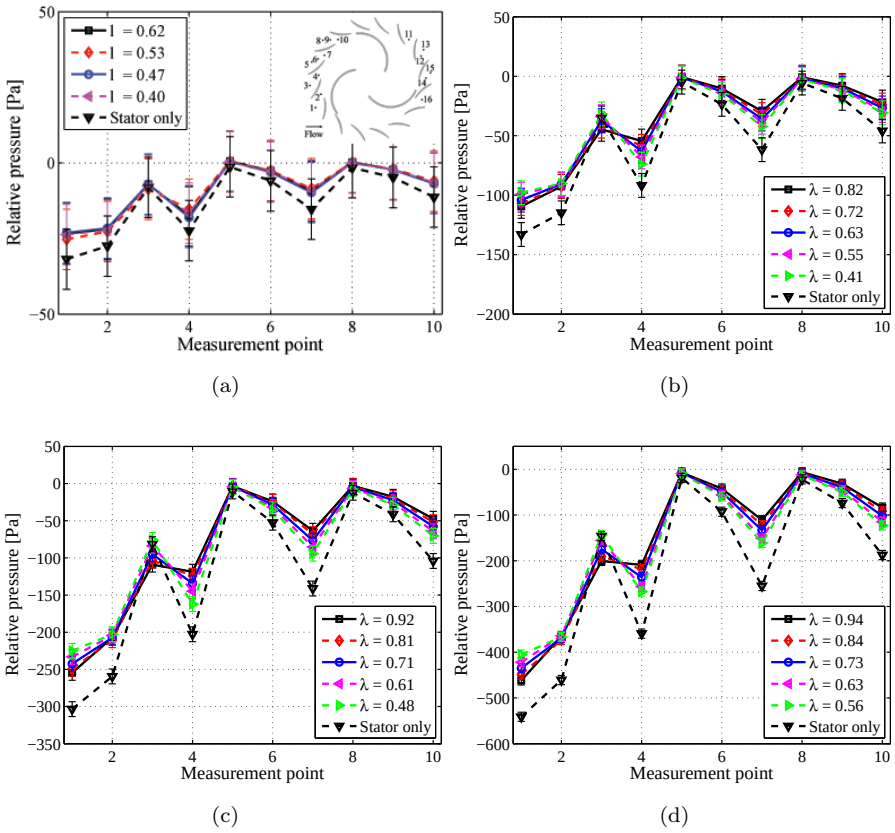

Figure 11: The effect of the tip-to-speed ratio on the upstream pressure distribution at Reynolds numbers of (a) 221 600, (b) 443 200, (c) 664 700 and (d) 886 300.

4. Conclusions

This study presented an experimental and analytical analysis on vaned Savonius turbine performance at different operating conditions by including experimental results, both with and without a rotor. In addition to the new model validation data, the key findings were the following:

1. A new correlation was developed for the modelling of a vaned Savonius turbine performance map with different Reynolds numbers and tip-to-speed ratios with an achievable accuracy of ±5%.

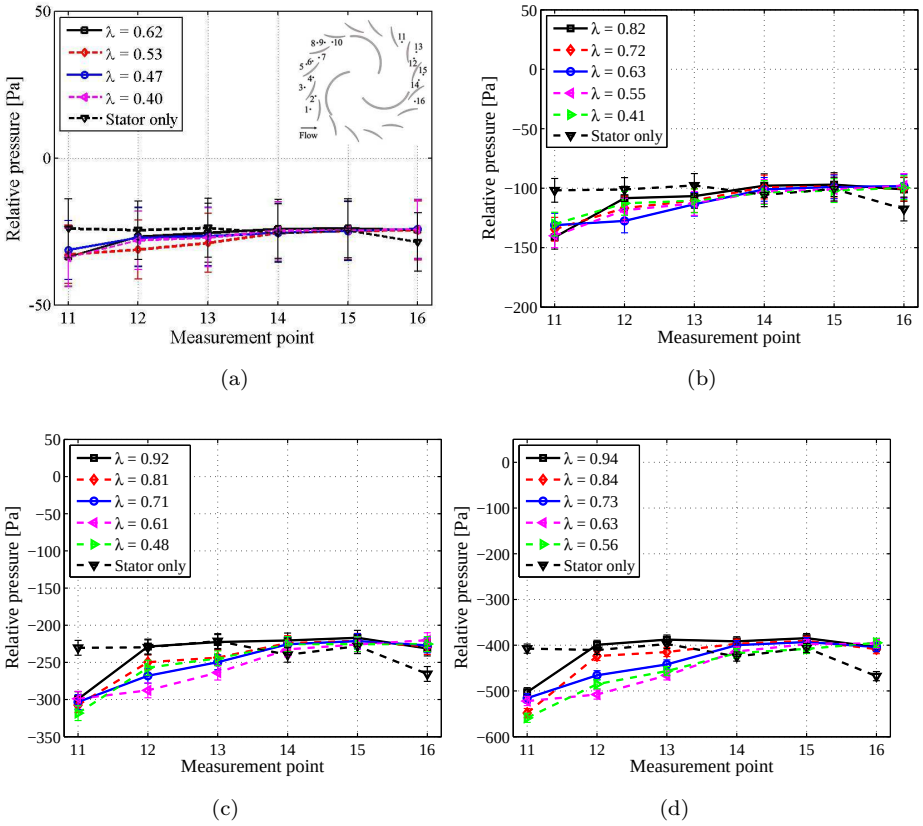

Figure 12: The effect of the tip-to-speed ratio on the downstream pressure distribution at Reynolds numbers of (a) 221 600, (b) 443 200, (c) 664 700 and (d) 886 300.

2. The effect of the Reynolds number on the Savonius turbine power coefficient follows the trend of kinetic compressors relatively well despite the existense of vanes, and an over 20% drop in vaned turbine power coefficient can be observed due to the changing Reynolds number.
3. The Reynolds number affects the performance both through the changing friction and flow separations, but it does not influence the vane passage pressure distribution shapes.
4. The tip-to-speed ratio influences the vane pressure distribution via the stator-rotor interaction.

It was also found that the stator-rotor interaction has opposing influences on the vane ring pressure distributions at the upstream and downstream parts of the turbine. At the upstream, the decrease of tip-to-speed ratio moves the pressure distribution closer to the case without stator-rotor interaction and vice versa at the downstream direction when the tip-to-speed ratio approaches 0.9. In the upstream, the behaviour is due to weaker interaction between the stator and rotor, whereas in the downstream, the behaviour is likely to be due to changes in the rotor-vortex interaction. However, there is a clear need for more data under different operating conditions in order to draw conclusions, and this could be a good avenue for further research.

In the context of performance prediction correlations, the data sets with different Savonius turbines seem to correlate well with C_T/Re^n as a function of tip-to-speed ratio. Therefore, it is also suggested that the reason for the found correlations is examined in future work.

It is suggested that in the design of vaned Savonius turbines, the tip-to-speed ratio at the nominal operating point should be kept relatively low, in order to minimise the negative effects of the stator-rotor interaction. Also, the influence of the Reynolds number on the peak performance point location should be taken into account.

In a broader view, the stator only results are also applicable for different turbine designs, such as H- and Bach-type rotors. It is reasonable to assume that the general trends in stator-rotor interaction can be found with other rotor designs as well, although the magnitude may be different due to variations in the tip-to-speed ratio and blade number.

Acknowledgements

The experimental campaign was funded and supported by Pasatel Oy. The authors acknowledge their co-operation during the project and thank them for granting permission to publish the results. Also, the support for the experiments from Arteform Oy was highly appreciated.

References

[1] A. Grönman, J. Backman, M. Laaksonen, M. Alkki, P. Aura, Experimental and numerical analysis of vaned wind turbine performance and flow phenomena, Energy 159 (2018) 827–841.

[2] M. H. Mohamed, G. Janiga, E. Pap, D. Thévenin, Optimal blade shape of a modified Savonius turbine using an obstacle shielding the returning blade, Energy Conversion and Management 52 (2011) 236–242.

[3] W. T. Chong, A. Fazlizan, S. C. Poh, K. C. Pan, W. P. Hew, F. B. Hsiao, The design, simulation and testing of an urban vertical axis wind turbine with the omni-direction-guide-vane, Applied Energy 112 (2013) 601–609.

[4] W. T. Chong, , K. C. Pan, S. C. Poh, A. Fazlizan, C. S. Oon, A. Badarudin, N. Nik-Ghazali, Performance investigation of a power augmented vertical axis wind turbine for urban high-rise application, Renewable Energy 51 (2013) 388–397.

[5] A. J. Alexander, B. P. Holownia, Wind tunnel tests on a Savonius rotor, Journal of Wind Engineering and Industrial Aerodynamics 3 (1978) 343–351.

[6] B. Shahizare, N. Nik-Ghazali, W. T. Chong, S. Tabatabaeikia, N. Izadyar, A. Esmaeilzadeh, Novel investigation of the different omni-direction-guide-vane angles effects on the urban vertical axis wind turbine output power via three-dimensional numerical simulation, Energy Conversion and Management 117 (2016) 206–217.

[7] R. Nobile, M. Vahdati, J. F. Barlow, A. Mewburn-Crook, Unsteady flow simulation of a vertical axis augmented wind turbine: A two-dimensional study, Journal of Wind Engineering and Industrial Aerodynamics 125 (2014) 168–179.

[8] M. Tartuferi, V. D'Alessandro, S. Montelpare, R. Ricci, Enhancement of Savonius wind rotor aerodynamic performance: A computational study of new blade shapes and curtain systems, Energy 79 (2015) 371–384.

[9] B. D. Altan, M. Atilgan, An experimental and numerical study on the improvement of the performance of Savonius wind rotor, Energy Conversion and Management 49 (2008) 3425–3432.

[10] K. Irabu, J. Roy, Characteristics of wind power on Savonius rotor using a guide-box tunnel, Experimental Thermal and Fluid Science 32 (2007) 580–586.

[11] N. Korprasertsak, T. Leephakpreeda, Analysis and optimal design of wind boosters for vertical axis wind turbines at low wind speed, Journal of Wind Engineering and Industrial Aerodynamics 159 (2016) 9–18.

[12] T. Hayashi, Y. Li, Y. Hara, Wind tunnel experiments of a newly developed two-bladed Savonius-style wind turbine, JSME International Journal, Series B 48 (2005) 9–16.

[13] W. T. Chong, W. K. Muzammil, K. H. Wong, C. T. Wang, M. Gwani, Y. J. Chu, S. C. Poh, Cross axis wind turbine: Pushing the limit of wind turbine technology with complementary design, Applied Energy 207 (2017) 78–95.

[14] M. Takao, H. Kuma, T. Maeda, Y. Kamada, M. Oki, A. Minoda, A straight-bladed vertical axis wind turbine with a directed guide vane row - Effect of guide vane geometry on the performance, Journal of Thermal Science 18 (2009) 54–57.

[15] L. Galanti, A. F. Massardo, Micro gas turbine thermodynamic and economic analysis up to 500 kWe size, Applied Energy 88 (2011) 4795–4802.

[16] F. Dietmann, M. Casey, The effects of Reynolds number and roughness on compressor performance, in: Proceedings of the 10th European Turbomachinery Conference, April 15-19, Lappeenranta, Finland, 2013.

[17] J. Tiainen, A. Jaatinen-Värri, A. Grönman, J. Backman, Influence of Reynolds number variation method on centrifugal compressor loss generation, in: Proceedings of 12th European Conference on Turbomachinery Fluid Dynamics and Thermodynamics, April 3-7, 2017, Stockholm, Sweden, no. ETC2017-041.

[18] J. Tiainen, A. Jaatinen-Värri, A. Grönman, T. Fischer, J. Backman, Loss development analysis of a micro-scale centrifugal compressor, Energy Conversion and Management 166 (2018) 297–307.

[19] B. F. Blackwell, R. E. Sheldahl, L. V. Feltz, Wind tunnel performance data for two- and three-bucket Savonius rotors, Tech. Rep. SAND76-0131, Sandia Laboratories (1977).

[20] J. V. Akwa, H. A. Vielmo, A. P. Petry, A review on the performance of Savonius wind turbines, Renewable and Sustainable Energy Reviews 16 (2012) 3054–3064.

[21] A. Al-Faruk, A. Sharifian, Geometrical optimization of a swirling Savonius wind turbine using an open jet wind tunnel, Alexandria Engineering Journal 55 (2016) 2055–2064.

[22] S. Roy, U. K. Saha, Wind tunnel experiments of a newly developed two-bladed Savonius-style wind turbine, Applied Energy 137 (2015) 117–125.

[23] M. A. Kamoji, S. B. Kedare, S. V. Prabhu, Performance tests on helical Savonius rotors, Renewable Energy 34 (2009) 521–529.

[24] M. A. Kamoji, S. B. Kedare, S. V. Prabhu, Experimental investigations on single stage modified Savonius rotor, Applied Energy 86 (2009) 1064–1073.

[25] J. M. Mercado-Colmenero, M. A. Rubio-Paramio, F. Guerrero-Villar, C. Martin-Doñate, A numerical and experimental study of a new Savonius wind rotor adaptation based on product design requirements, Energy Conversion and Management 158 (2018) 210–234.

[26] L. Wang, R. W. Yeung, On the performance of a micro-scale bach-type turbine as predicted by discrete-vortex simulations, Applied Energy 183 (2016) 823–836.

[27] N. Han, D. Zhao, J. U. Schluter, E. S. Goh, H. Zhao, X. Jin, Performance evaluation of 3D printed miniature electromagnetic energy harvesters driven by air flow, Applied Energy 178 (2016) 672–680.

[28] D. Zhao, N. Han, Optimizing overall energy harvesting performances of miniature Savoniuslike wind harvesters, Energy Conversion and Management 178 (2018) 311–321.

[29] M. Burlando, A. Ricci, A. Freda, M. P. Repetto, Numerical and experimental methods to investigate the behaviour of vertical-axis wind turbines with stators, Journal of Wind Engineering and Industrial Aerodynamics 144 (2015) 125–133.

[30] M. Virmavirta, J. Kivekäs, P. V. Komi, Take-off aerodynamics in ski jumping, Journal of Biomechanics 34 (2001) 465–470.

[31] A. Grönman, P. Sallinen, J. Honkatukia, J. Backman, A. Uusitalo, Design and experiments of two-stage intercooled electrically assisted turbocharger, Energy Conversion and Management 111 (2016) 115–124.

[32] K. Pope, V. Rodrigues, R. Doyle, A. Tsopelas, R. Gravelsins, G. F. Naterer, E. Tsang, Effects of stator vanes on power coefficients of a Zephyr vertical axis wind turbine, Renewable Energy 35 (2010) 1043–1051.

[33] H. Schlichting, Boundary layer theory, 7th Edition, McGraw-Hill, 1979.

[34] M. Torresi, B. Fortunato, G. Pascazio, S. M. Camporeale, CFD analysis of a Savonius rotor in a confined test section and open field, in: Proceedings of ASME Turbo Expo, June 6-10, Vancouver, British Columbia, Canada, GT2011-45877, 2011.